Finite calculation of divergent self-energy diagrams

A. Aste and D. Trautmann

Abstract: Using dispersive techniques, it is possible to avoid ultraviolet divergences in the calculation of Feynman diagrams, making subsequent regularization of divergent diagrams unnecessary. We give a simple introduction to the most important features of such dispersive techniques in the framework of the so-called finite causal perturbation theory. The method is also applied to the "divergent" general massive two-loop sunrise self-energy diagram, where it leads directly to an analytic expression for the imaginary part of the diagram in accordance with the literature, whereas the real part can be obtained by a single integral dispersion relation. It is pointed out that dispersive methods have been known for decades and have been applied to several nontrivial Feynman diagram calculations.

PACS Nos.: 11.10.–z, 11.15.Bt, 12.20.Ds, 12.38.Bx

Résumé : Utilisant des techniques dispersives, il est possible d'éviter les divergences ultraviolettes dans le calcul des diagrammes de Feynman, rendant inutile la régularisation des diagrammes divergents. Nous présentons de façon simple les caractéristiques les plus importantes de ces techniques dispersives dans le cadre de la théorie connue sous le nom de perturbation causale finie. Nous appliquons aussi la méthode aux diagrammes divergents de self énergie *soleil levant* à deux boucles où elle mène directement à une expression analytique pour la partie imaginaire du diagramme, en accord avec ce que dit la littérature, alors que la partie réelle peut être obtenue d'une simple relation de dispersion intégrale. Nous soulignons que les méthodes dispersives sont connues depuis des décennies et ont déjà été appliquées au calcul de plusieurs diagrammes de Feynman non triviaux.

[Traduit par la Rédaction]

1. Introduction

In quantum field theory, one usually starts from fields and a Lagrangean that describes the interaction. These objects get quantized and S-matrix elements or Greens functions are then constructed with the help of Feynman rules. However, these Feynman rules lead to products of distributions with singular behavior. This leads to the well-known ultraviolet divergences in perturbation theory. The occurrence of such divergences has led to the invention of several ingenious formal procedures such as Pauli–Villars regularization [1] or dimensional regularization [2]. The situation has remained not entirely satisfactory for several decades. So Feynman in his Nobel lecture remarked: "I think that the renormalization theory is simply a way to sweep the difficulties of the divergences of quantum electrodynamics under the rug."

Received 30 July 2003. Accepted 22 October 2003. Published on the NRC Research Press Web site at http://cjp.nrc.ca/ on 23 December 2003.

A. Aste[1] **and D. Trautmann.** Institute for Theoretical Physics, Klingelbergstrasse 82, Basel, Switzerland.

[1] Corresponding author (e-mail: aste@quasar.physik.unibas.ch).

 doi: 10.1139/P03-103

Today, the situation is not as bad as Feynman described it. The regularization procedures that remove infinities from the theory are well understood and it has become clear that UV divergences do not imply an inconsistency of the theory in general, but are a consequence of our current perturbative formulation of quantum field theories. Renormalization-group methods also shed a new light on their interpretation.

It is still widely unknown that it is possible to treat Feynman diagrams in such a manner that ultraviolet (UV) divergences do not appear in the calculations. This can be achieved by making explicit use of the causal structure of quantum field theory, i.e., by using dispersive techniques. Contrary to widespread belief, the use of dispersion relations in practical calculations is not unusual and has been employed by various authors in phenomenologically important evaluations of calculationally demanding quantum electrodynamic corrections such as higher order binding corrections to the two-loop bound-state quantum electrodynamic self-energy. Artru et al. used dispersive techniques as early as 1966 for a leading-order calculation of the Lamb shift [3, 4]. Pachucki has employed these relations for the evaluation of higher order binding corrections to the two-loop Lamb shift [5], and mentioned in his paper that the ultraviolet divergences canceled automatically in the calculations.

A very natural and rigorous approach to axiomatic perturbation theory, which has been applied successfully to all relevant interactions of the Standard model [6–8] and supersymmetric models [9,10], was provided by a classic paper of Epstein and Glaser in 1971 [11, 12]. Their method, called finite causal perturbation theory, or FCPT for short in this paper, avoids UV divergences from the start by defining mathematically correct time-ordered products for distributions. The resulting distributions are smeared out by test functions, avoiding provisional volume and infrared divergences at once. An extensive introduction to the causal method can be found in the textbook of Scharf on finite quantum electrodynamics [13]. There is now, also, a growing interest in FCPT, because it allows us to formulate a consistent renormalization theory on a curved physical background [14].

Basically, FCPT provides a clearly defined strategy for the dispersive calculation of Feynman diagrams. It renders all diagrams finite, but does not automatically solve problems related to the specification of normalization conditions and possible anomalies arising in the regularization procedure, which may violate symmetries that are necessary to give physical meaning. These problems like, for example, the formulation of Ward identities or the introduction of interacting fields in the framework of FCPT have been rated in recent years [15–19].

In FCPT, the Ansatz for the S matrix as a power series in the coupling constant is crucial, namely, S is considered as a sum of smeared operator-valued distributions

$$S(g) = \mathbf{1} + \sum_{n=1}^{\infty} \frac{1}{n!} \int \mathrm{d}^4x_1 \ldots \mathrm{d}^4x_n \, T_n(x_1, \ldots, x_n) \, g(x_1) \cdot \ldots \cdot g(x_n) \tag{1}$$

where the Schwartz test function $g \in \mathcal{S}(\boldsymbol{R}^4)$ switches the interaction and provides the infrared cutoff. The basic formulation of causality in FCPT, which had already been used by Bogoliubov et al. [20], is

$$S(g_1 + g_2) = S(g_2)S(g_1) \tag{2}$$

if the support of $g_2(x)$ is later than $\operatorname{supp} g_1$ in some Lorentz frame (usually denoted by $\operatorname{supp} g_2 > \operatorname{supp} g_1$). The condition allows for the construction of the n-point distributions T_n as a well-defined "renormalized" time-ordered product expressed in terms of Wick monomials of free fields $:\mathcal{O}(x_1, \ldots, x_n):$

$$T_n(x_1, \ldots, x_n) = \sum_{\mathcal{O}} :\mathcal{O}(x_1, \ldots, x_n): \, t_n^{\mathcal{O}}(x_1 - x_n, \ldots, x_{n-1} - x_n) \tag{3}$$

where the $t_n^{\mathcal{O}}$ are C-number distributions. T_n is constructed inductively from the first-order $T_1(x)$, which describes the interaction among the quantum fields, and from the lower orders T_j, $j = 2, \ldots, n-1$ by means of Poincaré covariance and causality. The inductive construction of the n-point distributions

T_n can be considered as the main technical difference of the theory to other approaches, since all lower orders $T_1, ...T_{n-1}$ must be calculated first to construct T_n. But the commonly chosen form of T_n

$$T_n(x_1, ..., x_n) = \sum_{\pi} \Theta(x^0_{\pi_1} - x^0_{\pi_2}) \cdot ... \cdot \Theta(x^0_{\pi_{n-1}} - x^0_{\pi_n}) T_1(x_{\pi_1}) \cdot ... \cdot T_1(x_{\pi_n}) \tag{4}$$

where the sum runs over all $n!$ permutations, is not an unambiguous definition, since it contains the product of Heaviside distributions with other singular distributions. This leads to the well-known UV divergences in the calculation of Feynman diagrams. One can illustrate this fact by the following simple one-dimensional example. The product of a Heaviside distribution $\Theta(t)$ with a δ-distribution $\delta(t)$ or even its derivative $\delta'(t)$ is obviously not well-defined. The Fourier transforms of the distributions are

$$\hat{\Theta}(\omega) = -\frac{i}{\sqrt{2\pi}} \frac{1}{\omega - i0}, \quad \hat{\delta}'(\omega) = \frac{i\omega}{\sqrt{2\pi}} \tag{5}$$

The ill-defined product $(\Theta\delta')(t)$ goes over into a nonexisting convolution by Fourier transform

$$(\Theta\delta')(t) \to \frac{1}{2\pi}(\hat{\Theta} * \delta')(\omega) = \frac{1}{(2\pi)^2} \int_{-\infty}^{+\infty} \mathrm{d}\omega' \, \frac{\omega - \omega'}{\omega' - i0} \tag{6}$$

which is definitely "'UV divergent".

It is the aim of this paper to demonstrate how UV finite results are obtained in the framework of FCPT by avoiding problematic Feynman integrals. This is done in Sect. 2, where technical details are explained. In Sect. 3, the method is applied to the well-known introductory case of a scalar self-energy diagram, and in Sect. 4, we apply the method to the less trivial case of the two-loop sunrise diagram with arbitrary masses.

2. The method

We start our considerations with a scalar neutral massive field ϕ_m with mass m, which satisfies the free Klein–Gordon equation. It can be decomposed into a negative- and positive-frequency part according to

$$\phi_m(x) = \phi_m^-(x) + \phi_m^+(x) = (2\pi)^{-3/2} \int \frac{\mathrm{d}^3k}{\sqrt{2E}} \left[a(\boldsymbol{k})\, \mathrm{e}^{-ikx} + a^\dagger(\boldsymbol{k})\, \mathrm{e}^{ikx} \right] \tag{7}$$

where $E = \sqrt{\boldsymbol{k}^2 + m^2}$. The commutation relations for such a field are given by the Jordan–Pauli distributions

$$\left[\phi_m^\mp(x),\ \phi_m^\pm(y)\right] = -i\, D_m^\pm(x - y) \tag{8}$$

which have the Fourier transforms

$$\hat{D}_m^\pm(p) = (2\pi)^{-2} \int \mathrm{d}^4x\, D_m^\pm(x)\, \mathrm{e}^{ipx} = \pm\frac{i}{2\pi} \Theta(\pm p^0) \delta(p^2 - m^2) \tag{9}$$

Since the commutator

$$[\phi_m(x), \phi_m(y)] = -i\, D_m^-(x - y) - i\, D_m^+(x - y) =: -i\, D_m(x - y) \tag{10}$$

vanishes for spacelike distances $(x - y)^2 < 0$ due to the requirement of microcausality, it follows immediately that the Jordan–Pauli distribution D_m has *causal support*, i.e., it vanishes outside the closed forward and backward light cone

$$\operatorname{supp} D_m(x) \subseteq \overline{V}^- \cup \overline{V}^+ \tag{11}$$

$$\overline{V}^{\pm} = \{x \mid x^2 \geq 0,\ \pm x^0 \geq 0\} \tag{12}$$

A crucial observation is the fact that the retarded propagator is given in real space by the covariant formula

$$D_m^{\mathrm{ret}}(x) = \Theta(x^0) D_m(x) \tag{13}$$

which goes over into a convolution in momentum space

$$\hat{D}_m^{\mathrm{ret}}(p) = (2\pi)^{-2} \int \mathrm{d}^4k\, \hat{D}_m(k)\hat{\Theta}(p-k) \tag{14}$$

The Heaviside distribution $\Theta(x^0)$ could be replaced by $\Theta(vx)$ with an arbitrary vector $v \in V^+$ inside the forward lightcone. The Fourier transform of the Heaviside distribution $\Theta(x^0)$ can be easily calculated

$$\hat{\Theta}(p) = (2\pi)^{-2} \lim_{\epsilon\to 0} \int \mathrm{d}^4x\, \Theta(x^0)\, \mathrm{e}^{-\epsilon x^0}\, \mathrm{e}^{ip_0x^0 - i\boldsymbol{px}} = \frac{2\pi i}{p^0 + i0}\delta^{(3)}(\boldsymbol{p}) \tag{15}$$

For the special case where p is in the forward light cone $\overline{V}^+$, we can go to a Lorentz frame where $p = (p^0, \mathbf{0})$ $(= p^0 = p_0$ as a shorthand) such that (14) becomes

$$\hat{D}_m^{\mathrm{ret}}(p^0) = \frac{i}{2\pi} \int \mathrm{d}k^0 \frac{\hat{D}_m(k^0)}{p^0 - k^0 + i0} = \frac{i}{2\pi} \int \mathrm{d}t\, \frac{\hat{D}_m(tp^0)}{1 - t + i0} \tag{16}$$

For arbitrary $p \in V^+$, $\hat{D}_m^{\mathrm{ret}}$ is, therefore, given by the *dispersion relation*

$$\hat{D}_m^{\mathrm{ret}}(p) = \frac{i}{2\pi} \int \mathrm{d}t\, \frac{\hat{D}_m(tp)}{1 - t + i0} \tag{17}$$

It is trivial but instructive to perform the actual calculation of $\hat{D}_m^{\mathrm{ret}}$. Exploiting the δ distribution in

$$\hat{D}_m(p) = \frac{i}{2\pi} \mathrm{sgn}(p^0)\delta(p^2 - m^2) \tag{18}$$

we obtain

$$\begin{aligned}
\hat{D}_m^{\mathrm{ret}}(p) &= -\frac{1}{(2\pi)^2} \int \mathrm{d}t\, \frac{\mathrm{sgn}(tp^0)\delta(t^2p^2 - m^2)}{1 - t + i0} \\
&= -\frac{1}{(2\pi)^2} \int \mathrm{d}t\, \frac{\left[\delta(t - \frac{m}{\sqrt{p^2}}) - \delta(t + \frac{m}{\sqrt{p^2}})\right]}{2\sqrt{p^2}m(1 - t + i0)} \\
&= -\frac{1}{(2\pi)^2} \frac{1}{p^2 - m^2 + i0}
\end{aligned} \tag{19}$$

We recover the analytic expression for the Feynman propagator, which coincides with

$$\hat{D}_m^{\mathrm{ret}}(p) = \hat{D}_m^F(p) + \hat{D}_m^-(p) = -\frac{1}{(2\pi)^2} \frac{1}{p^2 - m^2 + ip_0 0} \tag{20}$$

for $p \in V^+$. The imaginary part of the Feynman propagator is given by

$$\mathrm{Im}\,(\hat{D}_m^F(p)) = \frac{i}{4\pi}\delta(p^2 - m^2) \tag{21}$$

and can be deduced directly from the causal Jordan–Pauli distribution $\hat{D}_m$ in an obvious way.

2.1. The scalar one-loop self-energy diagram

As a first step, we define the causal distribution $\mathrm{d}(x-y)$ in conformity with (8) as the following vacuum expectation value of a massive and a massless field (the colons denote normal ordering)

$$(-i)\,\mathrm{d}(x-y) := \langle 0|[:\phi_m(x)\phi_o(x):,:\phi_m(y)\phi_o(y):]|0\rangle \tag{22}$$

which has again causal support due to microcausality. It is sufficient to consider

$$(-i)\,r(x-y) := -\langle 0|:\phi_m(y)\phi_o(y)::\phi_m(x)\phi_o(x):|0\rangle = D_m^-(x-y)D_o^-(x-y) \tag{23}$$

since $\mathrm{d}(x-y) = r(x-y) - r(y-x)$. The product of the two Jordan–Pauli distributions in real space goes over into a convolution in momentum space

$$\hat{r}(p) = \frac{i}{(2\pi)^2}(\hat{D}_m^- * \hat{D}_o^-)(p) \tag{24}$$

such that $\hat{\mathrm{d}}(p) = \hat{r}(p) - \hat{r}(-p)$.

Since we do *not* calculate the *time-ordered* product of fields, the Feynman propagators are replaced by Jordan–Pauli distributions.

The integral appearing in (24) is readily evaluated if one exploits the δ-distribution stemming from the massless field contraction in

$$\hat{r}(p) = -\frac{i}{(2\pi)^4}\int \mathrm{d}^4q\,\Theta(-q^0)\delta(q^2)\Theta(q^0-p^0)\delta((p-q)^2-m^2) \tag{25}$$

$\hat{r}(p)$ vanishes outside the closed backward light cone due to Lorentz invariance and the two Θ distributions in (25). Therefore, we can go to a Lorentz frame where $p = (p^0 < 0, \mathbf{0})$, and using the abbreviation $E = \sqrt{(\boldsymbol{q}^2 + m_1^2)}$ leads to

$$\begin{aligned}\hat{r}\left(p^0\right) &= -\frac{i}{(2\pi)^4}\int \frac{\mathrm{d}^3q}{2E}\delta\left(p_0^2 + 2p^0E - m^2\right)\Theta\left(-E-p^0\right)\\ &= -\frac{i}{2(2\pi)^3|p^0|}\int \mathrm{d}|\boldsymbol{q}||\boldsymbol{q}|\delta\left(\frac{p^0}{2} + E - \frac{m^2}{2p^0}\right)\Theta\left(-E-p^0\right)\\ &= -\frac{i}{2\,(2\pi)^3\,|p^0|}\Theta\left(-p^0\right)\Theta\left(p_0^2-m^2\right)\sqrt{\left(\frac{p^0}{2}-\frac{m^2}{2p^0}\right)^2}\end{aligned} \tag{26}$$

and for arbitrary p we get the intermediate result

$$\hat{r}(p) = -\frac{i}{32\pi^3}\frac{p^2-m^2}{p^2}\Theta\left(-p^0\right)\Theta\left(p^2-m^2\right) \tag{27}$$

Naive use of the dispersion relation (17) for the real part of the sunrise diagram would lead to an ultraviolet divergent expression. But it can be shown [13] that the finite part of the diagram is given for $p \in V^+$ by a subtracted dispersion relation (which is also called *splitting formula*)

$$\hat{t}^{\,\mathrm{ret}}(p) = \frac{i}{2\pi}\int_{-\infty}^{\infty}\mathrm{d}t\,\frac{\hat{\mathrm{d}}(tp)}{(t-i0)^{\omega+1}(1-t+i0)} \tag{28}$$

where ω is the power-counting degree of the diagram, which is in our case $\omega = 0$ since the diagram is logarithmically divergent. $\hat{t}^{\,\mathrm{ret}}(p)$ is normalized such that all derivatives of order $\leq \omega$ of $\hat{t}^{\,\mathrm{ret}}$ vanish at $p = 0$, i.e., in the present case

$$\hat{t}^{\,\mathrm{ret}}(0) = 0 \tag{29}$$

These statements are only meaningful if the derivatives of order $\leq \omega$ of $\hat{t}^{\,\mathrm{ret}}(p)$ exist in the sense of ordinary functions. This is assured in most cases by the existence of a massive field in the theory.

We mention here that (28) corresponds to the dispersion relation (113,10) used in the familiar textbook by Landau and Lifshitz on quantum electrodynamics [21].

Roughly speaking, the additional term in the denominator of (28) has a simple explanation. Writing (28) for $p = (p^0, \mathbf{0})$ as

$$\hat{t}^{\,\mathrm{ret}}(p^0) = \frac{i}{2\pi}(p^0)^{\omega+1} \int_{-\infty}^{\infty} \mathrm{d}k^0 \frac{\hat{\mathrm{d}}(k^0)}{(k^0 - i0)^{\omega+1}(p^0 - k^0 + i0)} \tag{30}$$

it becomes obvious that the division by $(k^0)^{\omega+1}$ acts as a kind of inverse differentiation on the causal distribution $\mathrm{d}(x)$ in real space. The transformed distribution has a less critical scaling behavior, and can be multiplied in a well-defined way by the time-ordering Θ distribution. After the splitting, the original part of $\mathrm{d}(x)$ in the forward light cone is recovered by differentiating $\omega + 1$ times along the time axis, corresponding to a multiplication of the distribution by $(p^0)^{\omega+1}$ in momentum space. This observation also shows the connection of the method to differential renormalization [22]. For further mathematical details we refer also to ref. 23.

The splitting integral can be evaluated by elementary methods

$$\hat{t}^{\,\mathrm{ret}}(p) = -\frac{1}{4(2\pi)^4} \int_{-\infty}^{\infty} \mathrm{d}t \, \frac{\mathrm{sgn}(t)\Theta(t^2p^2 - m^2)(t^2p^2 - m^2)}{t^3(1 - t + i0)\,p^2}, \qquad p \in V^+ \tag{31}$$

and leads directly to

$$\hat{t}(p) = \frac{1}{4(2\pi)^4}\left[\frac{m^2 - p^2}{p^2}\log\left(\frac{m^2 - p^2 - i0}{m^2}\right) + 1\right] \tag{32}$$

Distribution theory leaves the freedom to add a constant to the result, which corresponds to a local term $c_o\delta(x)$ in real space. Such local terms have to be restricted by further symmetry considerations in practical cases.

We arrived thus on a very direct way to a finite expression for the scalar one-loop self-energy diagram, which corresponds to a prefactor to the regularized expression of the Feynman integral

$$\int \frac{\mathrm{d}^4k}{(k^2 + i0)((p - k)^2 - m^2 + i0)} \tag{33}$$

We finally mention that one-loop diagrams in two space-time dimensions are treated in the framework of FCPT in ref. 24, whereas the three-dimensional QED is treated in ref. 13.

3. The sunrise diagram

In the following section, we will utilize the strategy discussed above for the calculation of the imaginary part of the sunrise diagram. This will show that the causal treatment of Feynman diagrams is also applicable to nontrivial cases. An extensive introduction to the calculation of two-loop diagrams in the causal method has been given in ref. 25, but the case of the sunrise diagram is missing there. Owing to the fundamental structure of the sunrise diagram, it is clear that it has been investigated using many different approaches, and in this paper it serves only as a convenient example of a dispersive calculation. We give, therefore, a short overview of the literature that is related to the subject in what follows.

There is now an increased interest in the precise calculation of multiloop Feynman diagrams. In the general massive case, relevant for future high-precision calculations in the electroweak theory,

Fig. 1. The general massive two-loop sunrise self-energy diagram.

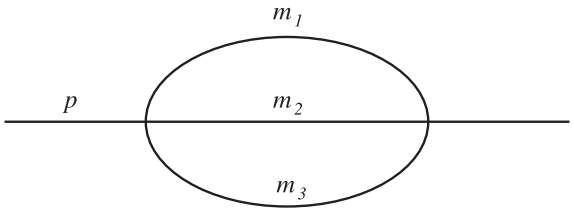

which go beyond the currently available one-loop electroweak radiative corrections [26], the number of parameters makes it impossible to obtain results in the usual analytic form. This negative result applies also to the case of the two-loop sunrise self-energy diagram shown in Fig. 1 with three different masses. When one or two internal particles are massless, the four-dimensional results can be obtained in terms of dilogarithms [27–30]. The situation is more complicated when all the virtual particles in the diagram have (different) masses. Such a situation occurs, for example, in the two-loop off-shell contributions to the Higgs self-energy. In three dimensions, the expression for the sunrise diagram is quite compact even for different masses [31], but in four dimensions, there are arguments [32] that the result cannot be expressed in terms of polylogarithms or other well-known special functions.

There is nowadays a widely accepted procedure for expressing radiative correction calculations in terms of a limited number of master integrals (MI) [33], which reduce the problem of finding analytic expressions for two-loop diagrams to the careful determination of the MI. The method also has the advantage that, with the correct bookkeeping of the recurrence relations arising from integration by parts identities, the MI of a given problem can be reused in more complicated calculations.

As already mentioned, the analytical calculation of MI (in terms of the usual polylogarithms and their generalizations) is possible only in cases with high symmetry, i.e., when the number of different scales (internal masses and external momenta or Mandelstam variables) is small as in QCD calculations, where all masses are set to zero; or in QED-type cases, where only the electron mass is different from zero; or when the external variables are fixed to particular values (zero or mass shell condition). Another possibility of help in analytic calculation is sometimes offered by the exploitation of particular simplifying conditions, like the smallness of some ratios of the parameters allowing the corresponding expansion.

The MI of the sunrise diagram were recognized to be expressible in closed form as a combination of four Lauricella functions, a special class of a generalized hypergeometric series, see ref. 34 and references therein. The method provides efficient multiple-series expansions for the regions of small $|p^2|$, i.e., $|p^2| < \max(m_i^2)$, and of large $|p^2| \gg (m_1 + m_2 + m_3)^2$, but some problems arise in the intermediate region.

There were also efforts devoted to the investigation of properties at special points (i.e., at $p^2 = 0,\ \infty$, pseudothresholds, and threshold). The analytical expansions of the MI at 0 and ∞ are given in refs. 34 and 35; the values at pseudothresholds and threshold in ref. 36; the analytical expansions at pseudothresholds can be found in ref. 37; a semi-analytical expansion at threshold in ref. 38 and also in configuration space technique in ref. 39, while the complete analytical expansions at threshold are presented in ref. 40.

For numerical evaluation purposes, it is possible to cast the general massive self-energy diagram in a double integral representation and in the particular case of the sunrise diagram in a single integral representation, see refs. 25, 34, 41, 42 and references therein. The configuration space technique is also exploited in the numerical approach [34, 43]. In a recent approach rearrangements of the integrand, driven by the Bernstein–Tkachov theorem, are introduced to improve numerical convergence [44]. A different and interesting method is the use of the recurrence relations as difference equations to evaluate the MI numerically [45].

It is of general interest to provide the widest possible range of insight into the structure and analytic properties of multiloop diagrams. In the present paper, we exploit the causal structure of the sunrise diagram, which immediately leads to a straightforward evaluation of the imaginary part of the diagram by elliptic functions. The real part of the diagram can then be obtained from a single integral dispersion relation. The dispersive method works especially well for diagrams that depend only on one external momentum, although it has already been used for different kinds of cases.

As in the case of the one-loop self-energy diagram, we define the causal distribution $\mathrm{d}(x-y)$ according to (8) as the vacuum expectation value of three massive fields (the colons denote normal ordering)

$$(-i)\,d(x-y) := \langle 0|\left[:\phi_{m_1}(x)\phi_{m_2}(x)\phi_{m_3}(x):,:\phi_{m_1}(y)\phi_{m_2}(y)\phi_{m_3}(y):\right]|0\rangle \tag{34}$$

which has causal support. As for the one-loop case, we consider

$$\begin{aligned}(-i)\,r(x-y) :&= -\langle 0|:\phi_{m_1}(y)\phi_{m_2}(y)\phi_{m_3}(y)::\phi_{m_1}(x)\phi_{m_2}(x)\phi_{m_3}(x):|0\rangle \\ &= i\,D^-_{m_1}(x-y)D^-_{m_2}(x-y)D^-_{m_3}(x-y)\end{aligned} \tag{35}$$

since $d(x-y) = r(x-y) - r(y-x)$. The product of the three Jordan–Pauli distributions in real space goes over into a threefold convolution in momentum space

$$\hat{r}(p) = -\frac{1}{(2\pi)^4}\left(\hat{D}^-_{m_1} * \hat{D}^-_{m_2} * \hat{D}^-_{m_3}\right)(p) \tag{36}$$

such that $\hat{d}(p) = \hat{r}(p) - \hat{r}(-p)$.

The dispersion relation (17) for the real part of the sunrise diagram is given by the splitting formula $\left(p \in V^+\right)$

$$\hat{t}^{\mathrm{ret}}(p) = \frac{i}{2\pi}\int \mathrm{d}t\,\frac{\hat{d}(tp)}{(t-i0)^3(1-t+i0)} \tag{37}$$

since the power counting degree of the quadratically divergent diagram is in this case $\omega = 2$. $\hat{t}^{\mathrm{ret}}(p)$ is normalized such that all derivatives of order $\leq \omega$ of $\hat{t}^{\mathrm{ret}}$ vanish at $p = 0$

$$\hat{t}^{\mathrm{ret}}(0) = 0, \qquad \frac{\partial}{\partial p_\mu}\hat{t}^{\mathrm{ret}}(0) = 0, \qquad \frac{\partial^2}{\partial p_\mu \partial p_\nu}\hat{t}^{\mathrm{ret}}(0) = 0 \tag{38}$$

3.1. The imaginary part

We will now calculate the three-fold convolution of the Jordan–Pauli distributions in momentum space given by (36). First we evaluate

$$\begin{aligned}\hat{d}_{12}(p) &= \left(\hat{D}^-_{m_1} * \hat{D}^-_{m_2}\right)(p) \\ &= -\frac{1}{(2\pi)^2}\int \mathrm{d}^4q\,\Theta\left(-q^0\right)\delta\left(q^2-m_1^2\right)\Theta\left(q^0-p^0\right)\delta\left((p-q)^2-m_2^2\right)\end{aligned} \tag{39}$$

$\hat{d}_{12}(p)$ vanishes outside the closed backward lightcone due to Lorentz invariance and the two Θ distributions in (39). In a Lorentz frame where $p = (p^0 < 0, \mathbf{0})$, we obtain $(E = \sqrt{(\boldsymbol{q}^2 + m_1^2)})$

$$\begin{aligned}\hat{d}_{12}\left(p^0\right) &= -\frac{1}{(2\pi)^2}\int \frac{\mathrm{d}^3 q}{2E}\delta\left(p_0^2 + 2p^0 E + m_1^2 - m_2^2\right)\Theta\left(-E - p^0\right)\\ &= -\frac{1}{2(2\pi)|p^0|}\int \mathrm{d}|\boldsymbol{q}||\boldsymbol{q}|\delta\left(\frac{p^0}{2} + E + \frac{m_1^2 - m_2^2}{2p^0}\right)\Theta\left(-E - p^0\right)\\ &= -\frac{1}{2(2\pi)|p^0|}\Theta\left(-p^0\right)\Theta\left(p_0^2 - (m_1 + m_2)^2\right)\sqrt{\left(\frac{p^0}{2} + \frac{m_1^2 - m_2^2}{2p^0}\right)^2 - m_1^2}\end{aligned} \tag{40}$$

and for arbitrary p we get the intermediate result

$$\hat{d}_{12}(p) = -\frac{1}{8\pi p^2}\Theta\left(-p^0\right)\Theta\left(p^2 - (m_1 + m_2)^2\right)\sqrt{p^4 - 2\left(m_1^2 + m_2^2\right)p^2 + \left(m_1^2 - m_2^2\right)^2} \tag{41}$$

which is symmetric in m_1, m_2 and exhibits the typical two-particle threshold behavior. Applying (28) with $\omega = 0$ to $\hat{d}_{12}(p)$ would generate the retarded one-loop propagator for a diagram with masses m_1 and m_2. As a next step we calculate

$$\begin{aligned}\hat{r}(p) &= -\frac{1}{(2\pi)^4}\left(\hat{D}^-_{m_3} * \hat{d}_{12}\right)(p)\\ &= -\frac{i}{4(2\pi)^6}\int \mathrm{d}^4 q\,\Theta\left(-q^0\right)\delta\left(q^2 - m_3^2\right)\Theta\left(q^0 - p^0\right)\Theta\left((p-q)^2 - (m_1 + m_2)^2\right)\\ &\qquad\times \frac{\sqrt{(p-q)^4 - 2\left(m_1^2 + m_2^2\right)(p-q)^2 + \left(m_1^2 - m_2^2\right)^2}}{(p-q)^2}\end{aligned} \tag{42}$$

For $p = (p^0, \mathbf{0})$ we obtain $\left(E = \sqrt{\boldsymbol{q}^2 + m_3^2}\right)$

$$\begin{aligned}\hat{r}(p) &= -\frac{i}{4(2\pi)^6}\int \frac{\mathrm{d}^3 q}{2E}\frac{\Theta\left(-E - p^0\right)\Theta\left(p_0^2 + 2p_0 E + m_3^2 - (m_1 + m_2)^2\right)}{p_0^2 + 2p_0 E + m_3^2} I\left(p_0\right)\\ &= -\frac{i}{4(2\pi)^5}\Theta\left(-p^0\right)\Theta\left(p_0^2 - (m_1 + m_2 + m_3)^2\right)\\ &\qquad\times \int_{m_3}^{-(p^0/2) + \left((m_1+m_2)^2 - m_3^2\right)/2p^0} \mathrm{d}E\,\frac{\sqrt{E^2 - m_3^2}}{p_0^2 + 2p_0 E + m_3^2} I\left(p_0\right)\end{aligned} \tag{43}$$

$$I\left(p_0\right) = \left(\left(p_0^2 + 2p_0 E + m_3^2\right)^2 - 2\left(m_1^2 + m_2^2\right)\left(p_0^2 + 2p_0 E + m_3^2\right) + \left(m_1^2 - m_2^2\right)^2\right)^{1/2} \tag{44}$$

The integral (43) can be written in a compact manner if we substitute $s = p_0^2 + 2p_0 E + m_3^2$. Going back to arbitrary Lorentz frames by replacing p^0 by $-\sqrt{p^2}$ where necessary, we obtain the following representation of $\hat{r}(p)$:

$$\hat{r}(p) = -\frac{i}{16(2\pi)^5 p^2}\Theta\left(-p^0\right)\Theta\left(p^2 - (m_1 + m_2 + m_3)^2\right)\,J(p) \tag{45}$$

where

$$J(p) = \int_{s_1}^{s_4} \frac{\mathrm{d}s}{s} \sqrt{(s - s_1)\,(s - s_2)\,(s_3 - s)\,(s_4 - s)} \tag{46}$$

and the variables $s_2 < s_1 < s_4 < s_3$ are defined via

$$\begin{aligned} s_1 &= (m_1 + m_2)^2 \\ s_2 &= (m_1 - m_2)^2 \\ s_3 &= \left(\sqrt{p^2} + m_3\right)^2 \\ s_4 &= \left(\sqrt{p^2} - m_3\right)^2 \end{aligned} \tag{47}$$

The integral in (46) can be expressed by complete elliptic integrals E, K, and Π

$$J = \gamma_1 E(\alpha) + \gamma_2 K(\alpha) + \gamma_3 \Pi(\beta_1, \alpha) + \gamma_4 \Pi(\beta_2, \alpha) \tag{48}$$

where

$$\begin{aligned} \alpha &= \sqrt{\frac{(s_4 - s_1)\,(s_3 - s_2)}{(s_3 - s_1)\,(s_4 - s_2)}} \\ \beta_1 &= \frac{s_4 - s_1}{s_4 - s_2} \\ \beta_2 &= \frac{s_2\,(s_4 - s_1)}{s_1\,(s_4 - s_2)} \\ \gamma_1 &= \frac{1}{4}\left(\sum_i s_i\right) \sqrt{(s_3 - s_1)\,(s_4 - s_2)} \\ \gamma_2 &= \frac{1}{4}\sqrt{\frac{s_4 - s_2}{s_3 - s_1}}\,(s_1 - s_2)\,(s_1 - s_2 + 3s_3 + s_4) \\ \gamma_3 &= -\frac{1}{4}\frac{(s_1 - s_2)}{\sqrt{(s_4 - s_2)\,(s_3 - s_1)}}\left(\sum_i s_i^2 - 2\sum_{i<j} s_i s_j\right) \\ \gamma_4 &= -2\frac{s_4 s_3\,(s_1 - s_2)}{\sqrt{(s_4 - s_2)\,(s_3 - s_1)}} \end{aligned} \tag{49}$$

For the sake of convenience and clarity, we note the definition of the complete elliptic integrals

$$\begin{aligned} E(k) &= \int_0^1 \mathrm{d}t \sqrt{\frac{1 - k^2 t^2}{1 - t^2}} \\ K(k) &= \int_0^1 \frac{\mathrm{d}t}{\sqrt{\left(1 - t^2\right)\left(1 - k^2 t^2\right)}} \\ \Pi(\nu, k) &= \int_0^1 \frac{\mathrm{d}t}{\sqrt{\left(1 - t^2\right)\left(1 - k^2 t^2\right)\left(1 - \nu^2 t^2\right)}} \end{aligned} \tag{50}$$

E, K, and Π satisfy very many identities, therefore, it might be possible that an even more compact form can be found for J. The analytic expression for $\hat{d}(p)$ follows from $\hat{r}(p)$ simply by replacing $\Theta(-p^0)$ by $-\mathrm{sgn}(p^0)$, and the imaginary part of the sunrise diagram is given by

$$\mathrm{Im}\left(\hat{t}(p)\right) = \frac{i}{32(2\pi)^5 p^2}\Theta\left(p^2-(m_1+m_2+m_3)^2\right) J \tag{51}$$

The result is indeed fully symmetric under permutations of m_1, m_2, m_3, although this is not obvious from (48). But for the higher symmetry cases, J becomes quite simple. For $m_1 = 0, m_2 = m_3 = m$, J reduces to

$$J(p) = \frac{1}{2}\left(p^2+2m^2\right)\sqrt{p^2\left(p^2-4m^2\right)} \tag{52}$$

for $m_1 = m_2 = 0, m_3 = m$ we have

$$J(p) = \frac{1}{2}\left(p^2-m^2\right)\left(p^2+m^2\right) \tag{53}$$

and for $m_1 = m_2 = m_3 = 0$, J collapses to

$$J(p) = \frac{1}{2}p^4 \tag{54}$$

Applying (37) to (52) and (53) leads to the results mentioned in the Introduction, which are expressible by polylogarithms and associated functions. But the subtracted dispersion relation (37) does not work in the totally massless case, where one encounters an additional infrared divergence that requires additional regularization that can be derived also as a limit from the massive case. The solution in the massless case, relevant, e.g., for QCD or quantum gravity, is

$$\hat{t}^{\mathrm{ret}}\left(p^2\right) = \hat{t}\left(p^2\right) + \hat{r}(p) = -\frac{1}{32(2\pi)^6}p^2\log\frac{-\left(p^2+ip_00\right)}{M^2} \tag{55}$$

$$\hat{t}\left(p^2\right) = -\frac{1}{32(2\pi)^6}p^2\log\frac{-\left(p^2+i0\right)}{M^2} = -\frac{1}{32(2\pi)^6}p^2\left(\log\left|\frac{p^2}{M^2}\right| - i\pi\Theta\left(p^2\right)\right) \tag{56}$$

with a real scaling parameter M. Equation (56) reflects also the high-energy behavior of the massive propagator $\hat{t} \sim p^2\log(p^2)$. The prefactor $(2\pi)^{-6}$ in the expressions above is due to the fact that we have included a prefactor $(2\pi)^{-2}$ in our definition of the Feynman propagator.

4. Final remarks and conclusion

A closed analytic expression has been derived for the imaginary part of the scalar sunrise diagram with arbitrary masses of the virtual particles. The technical difference between the usual Feynman-diagram calculations and the method used in the present paper is that the occurring integrals are reduced step by step to single integrals by utilizing the δ distributions in the Jordan–Pauli distributions instead of performing a Wick rotation. The real part of the sunrise diagram can be expressed for all values of the external impulse by a single integral, because the causal distribution $\hat{d}$, which is related to the imaginary part of the diagram and has the special form

$$\hat{d}(p) = h\left(p^2\right)\mathrm{sgn}\left(p^0\right)\Theta\left(p^2-m_{\mathrm{tot}}^2\right), \qquad m_{\mathrm{tot}} = m_1+m_2+m_3 \tag{57}$$

therefore, the dispersion relation (37) can also be written for $p \in V^+$

$$\hat{r}^{\mathrm{ret}}(p) = \hat{t}(p) + \hat{r}(p) = \frac{i}{2\pi}\left(p^2\right)^{[\omega/2]+1}\int_{m_{\mathrm{tot}}^2}^{\infty}\mathrm{d}s\,\frac{h(s)}{s^{[\omega/2]+1}\left(p^2-s+ip_00\right)} \tag{58}$$

where $[\omega/2]$ denotes the largest integer $\leq \omega/2$. This formula can be extended to space-like p by analytic continuation

$$\hat{r}^{\mathrm{ret}}\left(p^2\right) = \frac{i}{2\pi}\left(-p^2\right)^{[\omega/2]+1} \int\limits_{m_{\mathrm{tot}}^2}^{\infty} \mathrm{d}s \, \frac{h(s)}{s^{[\omega/2]+1}\left(-p^2-s\right)} \tag{59}$$

such that that an access to numerical and analytic investigations is provided for the whole range of external momenta.

The problem of overlapping divergences is automatically solved by the causal method due to the inductive construction of the theory, whereas in usual renormalization schemes, it becomes a nontrivial problem to show that all subdiagrams of a given diagram can be renormalized in a consistent way. In the context of the BPHZ (Bololiubov–Parasiuk–Hepp–Zimmerman) method [46–48], the problem was solved using the forest formula, an algorithm that disentangles all divergences in subdiagrams [49]. This is one of the conceptual strengths of the causal approach. Furthermore, it should be pointed out that on the level of the sunrise diagram discussed in this paper, the calculation of the imaginary part can as well be understood by the Cutkoski rules. But at higher orders, one should clearly distinguish between these rules that rely mainly on the unitarity of the theory, whereas in the causal approach the main input is causality.

We have used the example of the surise diagram to illustrate, in a pedagogical manner, the strategy and fundamental properties of the dispersive approach for the calculation of Feynman diagrams. We refer also to the recent literature on the specific case of the sunrise diagram, where also nontrivial vertex structures are treated by dispersive and nondispersive methods [42, 50, 51].

References

1. W. Pauli and F. Villars. Rev. Mod. Phys. **21**, 434 (1949).
2. G.'t Hooft and B. Veltmann. Nucl. Phys. **B44**, 189 (1972).
3. X. Artru, J.L. Basdevant, and R. Omnes. Phys. Rev. **150**, 1387 (1966).
4. H.D.I. Abarbanel. Ann. Phys. **39**, 177 (1966).
5. K. Pachucki. Phys. Rev. Lett. **72**, 3154 (1994).
6. A. Aste and G. Scharf. Int. J. Mod. Phys. A, **14**, 3421 (1999).
7. A. Aste, G. Scharf, and M. Dütsch. Annalen Phys. **8**, 389 (1999).
8. N. Grillo. Ann. Phys. **287**, 153 (2001).
9. F. Constantinescu, M. Gut, and G. Scharf. Annalen Phys. **11**, 335 (2002).
10. D.R. Grigore. Eur. Phys. J. C, **21**, 723 (2001).
11. H. Epstein and V. Glaser. Annales Poincaré Phys. Theor. A, **19**, 211 (1973).
12. H. Epstein and V. Glaser. Le rôle de la localité dans la renormalisation perturbative en théorie quantique des champs. Statistical mechanics and quantum field theory. (Les Houches 1970.) Gordon and Breach, New York. 1971.
13. G. Scharf. Finite quantum electrodynamics. 2nd ed. Springer Verlag, New York. 1995.
14. R. Brunetti and K. Fredenhagen. Commun. Math. Phys. **208**, 623 (2000).
15. M. Dütsch and K. Fredenhagen. Commun. Math. Phys. **203**, 71 (1999).
16. M. Dütsch and K. Fredenhagen. hep-th/0211242.
17. T. Hurth and K. Skenderis. Lect. Notes Phys. **558**, 86 (2000).
18. G. Barnich, M. Henneaux, T. Hurth, and K. Skenderis. Phys. Lett. B, **492**, 376 (2000).
19. G. Barnich, T. Hurth, and K. Skenderis. hep-th/0306127.
20. N.N. Bogoliubov and D.V. Shirkov. Introduction to the theory of quantized fields. Wiley-Interscience, London. 1959.
21. L.D. Landau and E.M. Lifshitz. Quantum electrodynamics. Pergamon Press, Oxford. (1983).
22. D. Prange. J. Phys. A, **32**, 2225 (1999).
23. J.M. Gracia-Bondia and S. Lazzarini. J. Math. Phys. **44**, 3863 (2003).
24. A. Aste, G. Scharf, and U. Walther. Nuovo Cimento Soc. Ital. Fis. A, **111**, 323 (1998).

25. A. Aste. Ann. Phys. **257**, 158 (1997).
26. A. Denner and S. Pozzorini. Eur. Phys. J. C, **21**, 63 (2001).
27. F.A. Berends and J.B. Tausk. Nucl. Phys. **B421**, 456 (1994).
28. G. Källén and A. Sabry. Dan. Mat. Fys. Medd. **29**, no. 17, 1 (1955).
29. D.J. Broadhurst, J. Fleischer, and O.V. Tarasov. Z. Phys. C, **60**, 287 (1993).
30. J. Fleischer, A.V. Kotikov, and O.L. Veretin. Nucl. Phys. **B547**, 343 (1999).
31. A.K. Rajantie. Nucl. Phys. **B480**, 729 (1996).
32. R. Scharf. Ph.D. thesis. University of Würzburg, Germany. 1994
33. F.V. Tkachov. Phys. Lett. **100B**, 65 (1981); K.G. Chetyrkin and F.V. Tkachov. Nucl. Phys. **B192**, 159 (1981).
34. F.A. Berends, M. Böhm, M. Buza, and R. Scharf. Z. Phys. C, **63**, 227 (1994).
35. M. Caffo, H. Czyż, S. Laporta, and E. Remiddi. Nuovo Cimento Soc. Ital. Fis. A, **111**, 365 (1998).
36. F.A. Berends, A.I.Davydychev, and N.I. Ussyukina. Phys. Lett. **426B**, 95 (1998).
37. M. Caffo, H. Czyż, and E. Remiddi. Nucl. Phys. **B581**, 274 (2000).
38. A.I. Davydychev and V.A. Smirnov. Nucl. Phys. **B554**, 391 (1999).
39. S. Groote and A.A. Pivovarov. Nucl. Phys. **B580**, 459 (2000).
40. M. Caffo, H. Czyż, and E. Remiddi. Nucl. Phys. **B611**, 503 (2001).
41. P. Post and J.B. Tausk. Mod. Phys. Lett. **11A**, 2115 (1996).
42. S. Bauberger, F.A. Berends, M. Böhm, and M. Buza. Nucl. Phys. **B434**, 383 (1995).
43. S. Groote, J.G. Körner, and A.A. Pivovarov. Eur. Phys. J. C, **11**, 279 (1999); Nucl. Phys. **B542**, 515 (1999).
44. G. Passarino. Nucl. Phys. **B619**, 257 (2001).
45. S. Laporta. Int. J. Mod. Phys. A, **15**, 5087 (2000); Phys. Lett. **504B**, 188 (2001).
46. N.N. Bogoliubov and O.S. Parasiuk. Acta Math. **97**, 227 (1957).
47. K. Hepp. Commun. Math. Phys. **2**, 301 (1996).
48. W. Zimmermann. Lectures on elementary particles and quantum field theory. Proc. Brandeis Summer Institute (1970). MIT Press, cambridge, Mass.
49. W. Zimmermann. Commun. Math. Phys. **15**, 208 (1969).
50. A.I. Davydychev and R. Delbourgo. hep-th/0209233.
51. A. Bashir, R. Delbourgo, and M.L. Roberts. J. Math. Phys. **42**, 5553 (2001).